Review

Cardiovascular Magnetic Resonance in Cardiomyopathy

M Dwornik, Z Khalique, R Rajakulasingam, AD Scott, A Azzu, PF Ferreira, S Nielles-Vallespin & DJ Pennell

Keywords
Cardiomyopathy, Cardiovascular magnetic resonance

Maria Dwornik[1,2]
MD
Research Fellow

Zohya Khalique[1,2]
MD, MBBS
Academic Clinical Lecturer

Ramyah Rajakulasingam[1,2]
MBBS
Research Fellow

Andrew D Scott[1,2]
PhD
Senior Physicist

Alessia Azzu[1,2]
MD
Research Fellow

Pedro F Ferreira[1,2]
PhD
Senior Physicist

Sonia Nielles-Vallespin[1,2]
PhD
Senior Physicist, Head of CMR Physics Department

Dudley J Pennell[1,2]
MD FRCP FACC FESC FRCR FAHA FMedSci FSCMR
Professor of Cardiology

[1] Royal Brompton Hospital (CMR Department)
Sydney Street
London
SW3 6NP
United Kingdom
[2] National Heart and Lung Institute, Imperial College London
Dovehouse Street
London
SW3 6LY
United Kingdom

Correspondence
Dudley Pennell
Royal Brompton Hospital
Sydney Street, London
SW3 6NP, UK
Email: dj.pennell@rbht.nhs.uk

Key Learning Points

- Cardiomyopathy is a common cause of heart failure and sudden cardiac death in young adults. Accurate cardiac phenotyping is key to the diagnosis, risk stratification and management of these patients. Cardiovascular magnetic resonance plays a central role in this process, uniquely providing multiparametric comprehensive cardiac evaluation.

Introduction

Cardiomyopathies are defined as "myocardial disorders in which the heart muscle is structurally and functionally abnormal, in the absence of attributable coronary artery disease, hypertension, heart valve or congenital heart disease".[1] This is an aetiologically and clinically diverse group of conditions, sharing important characteristics such as risk of sudden cardiac death (SCD) and possible heritable nature. Accurate phenotyping is key to the diagnosis and management for key probands and their relatives. Cardiovascular magnetic resonance (CMR) is central in this process, offering comprehensive multi-parametric assessment, enabling not only accurate phenotyping, but also identifying prognostic risk markers. We review the key aspects of CMR technique and the diagnostic and risk stratification applications of CMR in cardiomyopathy.

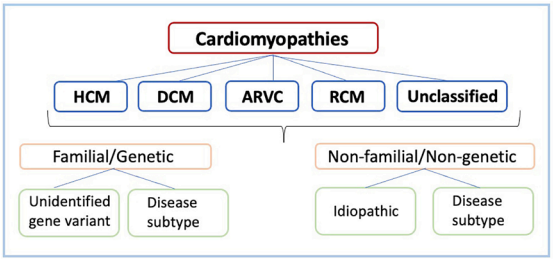

Figure 1. European Society of Cardiology (ESC) classification of cardiomyopathies (2008). This classification defines 5 distinct cardiomyopathy types: hypertrophic cardiomyopathy (HCM), dilated cardiomyopathy (DCM), arrhythmogenic right ventricular cardiomyopathy (ARVC), restrictive cardiomyopathy (RCM) and unclassified cardiomyopathy. Each of the cardiomyopathy types is sub-classified into familial and non-familial forms, highlighting possible genetic cause and heritable nature.

Classification of Cardiomyopathies

In 2008, European Society of Cardiology proposed a clinical classification of cardiomyopathies[1] (Figure 1) to replace the previous dichotomous terminology of primary and secondary cardiomyopathy. It is based primarily on accurate cardiac phenotyping. Such categorisation provides a pragmatic framework for clinicians to navigate the diagnostic pathway, which begins with identification of a specific phenotype, followed by a search for an underlying aetiology. CMR has emerged as one of the key tools enabling the use of this classification strategy.

Cardiovascular Magnetic Resonance

Technique

The discoveries leading to the development of CMR date back to 1946, when Felix Bloch and Edwin Purcell independently described the phenomenon of nuclear magnetic resonance (NMR)[2]. Further scientific discoveries allowed initial application of NMR in spectroscopy for *in vivo* molecular "imaging" of metabolism. In 1970, Paul Lauterbur described a method of image generation using NMR[3], the cardiac application of which was galvanised by the discovery of high-speed imaging by Peter Mansfield[4].

MRI (magnetic resonance imaging) utilises a signal generated by hydrogen atoms, each consisting of a single proton. Protons are contained in abundance within water and lipid molecules of biological tissues. Protons have an intrinsic property of nuclear spin, acting as small magnets. When placed in the strong static magnetic field,

the proton spins align parallel with that field. Application of a radiofrequency (RF) wave (pulse) tips the alignment of the protons. Upon removal of the RF pulse, the spins return to their original position, releasing energy, which is detected as a signal and transformed into an image. Gradual decay of signal following cessation of the RF pulse occurs with a time constant (T2) and the simultaneous, yet slower recovery of the net magnetisation occurs at a time constant (T1). Magnetic field inhomogeneities result in a faster signal decay than the intrinsic T2, which is described by the time constant T2 star (T2*). T1, T2 and T2* times vary by tissue composition, and these differences can be exploited to generate tissue contrast that enables tissue characterisation. CMR imaging requires several challenges to be overcome, such as motion (intrinsic and respiratory) and arrhythmias. Both free-breathing and breath-hold CMR sequences have been developed, enabling acquisition of high-quality cardiac images.

Clinical Applications relevant to Cardiomyopathy

CMR is now an established non-ionising and highly versatile cardiac imaging modality, enabling acquisition of cardiac views in any imaging plane. It benefits from excellent soft tissue contrast and endocardial definition, with a high inter-study and inter-operator reproducibility[5,6]. CMR offers a unique comprehensive cardiac evaluation in one study, encompassing assessment of cardiac anatomy and function, vascular anatomy, blood flow, myocardial perfusion and myocardial tissue characterisation. A detailed description of all underlying techniques is beyond the remit of this review, but key principles of anatomy, perfusion and tissue characterisation are discussed further.

Cardiovascular anatomy and function

There are two main categories of CMR images: static (acquired at a specific time point of cardiac cycle) or cine (a series of images acquired throughout the cardiac cycle, reflecting cardiac motion, perfusion or blood flow). The initial static images are acquired to locate the heart position in the chest are followed by a set of images to define chest anatomic outlines, major vessels and their connections. Importantly, these images are used to identify cardiac axes in an individual patient, allowing further tailored planning of dedicated static and cine images in standard or any required imaging planes. Cine images allow assessment of cardiac chamber volumes, regional function and ventricular ejection fraction[5,6]. Owing to high accuracy of measurements and excellent reproducibility[5,6], CMR is a gold standard method for cardiac mass and volumetric quantification[7].

Perfusion

CMR myocardial perfusion imaging utilises a method of "first pass perfusion" tracking the passage of contrast agent through the myocardium. This is performed at rest and during peak pharmacologic stress (achieved by infusion of a vasodilator). Adenosine stress perfusion CMR can identify myocardial perfusion abnormality without the use of ionising radiation[8,9]. Both qualitative and quantitative analysis possible with ischaemic burden assessment.

Gadolinium-based contrast agent (GBCA) utilisation in CMR

GBCAs are extracellular molecules (i.e. they do not cross intact cell membranes) and when injected intravenously, wash out from the capillary bed of tissues within minutes, but stay longer in the interstitial space (10-30 minutes), creating a window of opportunity for gadolinium enhancement imaging[8,9]. The latter are acquired using a T1-dependent inversion recovery sequence, utilising the property of GBCAs to shorten T1.

Early gadolinium enhancement (EGE) images are acquired within the first 10 minutes of contrast administration, giving a bright signal from the blood pool[10]. The regions lacking normal blood pool distribution appear darker compared to the brighter blood pool, indicating the presence of an avascular mass, such as an intracardiac thrombus. Detection of intracardiac thrombi has immediate ramifications for clinical care and is especially relevant in cardiomyopathy.

Late gadolinium enhancement (LGE) images are acquired 10 minutes after contrast administration, resulting in a hyper-intense signal of the myocardial regions with a delayed GBCA wash out (due to pathological processes), compared to the darker regions of normal myocardium. Such delayed myocardial GBCA wash out occurs in a wide range of pathological processes, such as cardiomyocyte injury, fibrotic scarring, expansion of extracellular space due to oedema, inflammation or infiltration. Validated methods have been developed for LGE quantification, expressed as percentage of LV myocardial mass or volume[11,12]. LGE has emerged as an in vivo imaging marker of myocardial fibrosis, becoming one of the key CMR tools of myocardial tissue characterisation[13]. Myocardial fibrosis is a histological marker common for many aetiologies of heart failure and is thought to be a substrate for arrhythmogenesis[14]. Its detection and quantification are important for both differential diagnosis and risk stratification across a range of cardiovascular diseases, including cardiomyopathy. There are two main types of histologically identifiable myocardial fibrosis: replacement (which occurs due to cardiomyocyte death and scarring) and interstitial (due to expansion of extracellular space in a variety of pathologic processes)[13]. CMR provides unique non-invasive in vivo myocardial tissue characterisation and reliably detects both replacement and interstitial fibrosis by LGE and T1 mapping methods respectively[15–17].

Myocardial T1, T2 and T2 Mapping Techniques*

Measurement of T1 relaxation times before GBCA administration (native) and in the LGE window (10-30 minutes post GBCA administration) has been proposed as a method of in vivo detection of interstitial fibrosis, which may be difficult to detect by LGE CMR[16,17]. The pre- and post-contrast T1 values can be used with a measurement of haematocrit to estimate myocardial extracellular volume fraction (ECV,%) which provides a measure of extracellular space expansion by

processes such as oedema, infiltration, fibrosis or abnormal protein deposition[16,17] (Figure 2).

T2-weighted sequences allow detection of myocardial regions with a relative increase in water content (i.e. oedema), which produces a hyperintense signal in comparison to the surrounding regions[18]. Myocardial oedema prolongs T2 times. The latter can be quantified using T2 mapping methods, with certain thresholds of T2 values denoting myocardial oedema. Myocardial oedema is present in pathologies, such as acute myocarditis or acute myocardial infarction. In pathologies with global myocardial involvement, oedema can be challenging to detect using regional tissue contrast methods, but the global myocardial signal intensity can be compared to that of skeletal muscle, with the ratio of ≥2 signifying myocardial oedema[18]. Furthermore, myocardial hyperaemia and capillary leak can manifest as increased early (imaged within first 3 minutes) gadolinium uptake on T1-weighted sequences with the ratio of global myocardial early enhancement signal intensity to that from skeletal muscle ≥4 signifying myocardial oedema[18].

T2* mapping utilises signal loss due to magnetic field inhomogeneities and the associated shortening of the signal decay time constant[9,19]. Measurement of T2* times is a validated gold standard method for early detection and quantification of cardiac iron load[20], validated against histology[21] and utilised in pathologies associated with cardiac and liver iron overload.

Evolving CMR Methodologies in Cardiomyopathy

CMR continues to evolve, unravelling new avenues for translational research into novel methodologies. One such methodology is diffusion weighted[22] and diffusion tensor CMR[23–25], which provide unique insights into human myocardial tissue integrity, architectural organisation and microstructure in vivo without the use of contrast. The final section below demonstrates examples of application in cardiomyopathy. Another non-contrast method enabling myocardial tissue composition assessment is T1ρ (rho) mapping, which uses distinct mechanisms of MR tissue contrast generation compared to that used in conventional T1 and T2 methods[26]. T1ρ imaging is sensitive to oedema and fibrosis and emerges to have a better corelation with markers of myocardial performance compared to T1 and T2 methods[27]. Furthermore, magnetic resonance properties of both hydrogen and non-hydrogen nuclei (for example, phosphorus, sodium or carbon) are utilised by cardiac MR spectroscopy[9]. This enables inferences to be made regarding molecular composition of myocardial tissue in health and disease, measuring for example the content of sodium (which is raised in acute myocardial injury) or metabolic components implicated in energy generation at a cellular level (with the ratio of phosphocreatine and adenosine triphosphate reduced in heart failure)[9]. All these techniques are under investigation and their future applications in cardiomyopathy is an area to be watched. Below we provide a summary of key CMR applications in the diagnosis and risk stratification of cardiomyopathy.

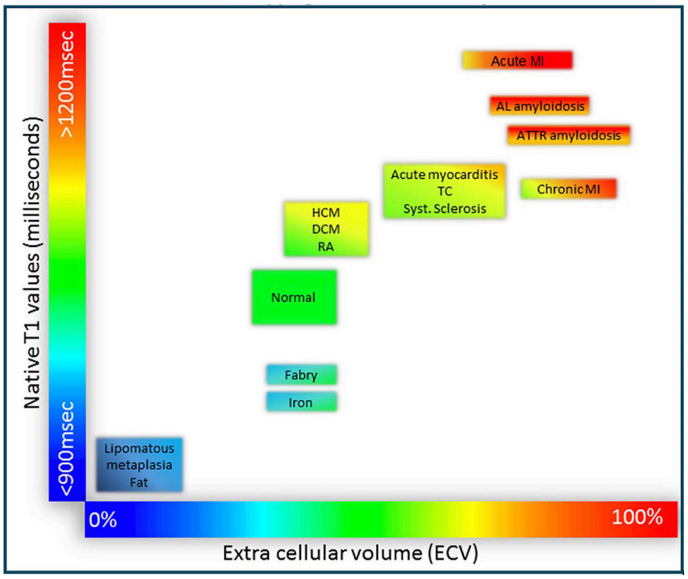

Figure 2. The role of CMR tissue characterisation using native T1 and extracellular volume (ECV) quantification in the differential diagnosis of cardiomyopathies. Absolute values of native T1 and ECV depend on the strength of magnetic field, scanner vendor and sequence used. Adapted from Philip Haaf and Martin Ugander (SCMR 2014)[16]. MI: myocardial infarction; AL: light chain amyloidosis; ATTR: transthyretin amyloidosis; TC: Takotsubo cardiomyopathy; RA: rheumatoid arthritis

Hypertrophic Cardiomyopathy (HCM)

Hypertrophic cardiomyopathy (HCM) is a common heritable heart muscle disease, affecting as many as 1:200 to 1:500 individuals in the general population and is associated with increased risk of sudden cardiac death (SCD)[28]. A genetic cause can be found in 30-60% of cases[29].

Definition.

Clinical diagnosis hinges on the identification of left ventricular hypertrophy (LVH) in the absence of abnormal loading conditions, systemic or infiltrative process sufficient to cause the observed magnitude of LVH[30,31]. Histological hallmarks of HCM are cardiomyocyte hypertrophy, significant cardiomyocyte disarray (>10% of myocardium), interstitial fibrosis and coronary arteriolar perivascular fibrosis and smooth muscle hyperplasia[32].

Phenotype.

LVH is the defining feature of HCM. It is typically asymmetric, focal and can affect any region of the left ventricle (LV), resulting in diverse morphologic forms of HCM[33]. The classic description is of asymmetric septal hypertrophy with small LV cavity, supranormal LV ejection fraction (LVEF), systolic anterior motion of mitral valve leaflet towards the septum (SAM) and resultant left ventricular outflow tract obstruction (LVOTO), Figure 3. The latter is a marker of risk[28] and identifiable at rest in 30% of HCM cases, while further 30% have provocable LVOTO (with Valsalva manoeuvre or exercise)[30]. A proportion of patients (~10%) have LVH affecting mainly mid-apical LV ("apical HCM") with resultant intra-cavity obstruction and risk of LV apical aneurysm formation and thromboembolic

Cardiovascular Magnetic Resonance in Cardiomyopathy

complications[30]. Concentric LVH is rare in HCM[33]. Owing to the wide imaging field, excellent endocardial border definition and ability to acquire tomographic non-oblique views of LV short axis, CMR is superior to echocardiography in the accuracy of LV evaluation, including in the antero-lateral[34] and apical[35] segments where echocardiography can miss pathology altogether. The degree of hypertrophy is an independent predictor of risk, hence accurate assessment is critically important[28].

Despite often supranormal LVEF, HCM subjects have reduced myocardial contractility which can be assessed using CMR strain imaging methods that show abnormal strain characteristics[36,37].

Around 30% of HCM subjects have severe coronary microvascular ischaemia in the absence of coronary artery disease[38], which is thought to aggravate disease progression and may be a marker of risk[39].

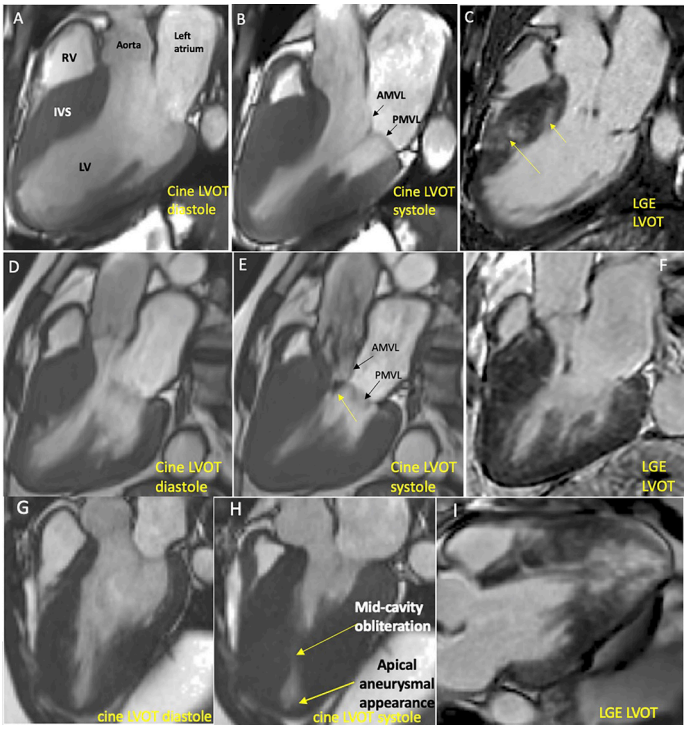

Figure 3. CMR in hypertrophic cardiomyopathy. Case 1 (images A-C): asymptomatic 27-year-old man referred for CMR due to family history of HCM. CMR revealed severe (24 mm) asymmetric septal hypertrophy (A) with no SAM or LVOTO on rest (B) and patchy mid-wall myocardial fibrosis in the hypertrophied septum (C). Case 2 (images D-F): 67-year-old woman with severe exertional dyspnoea and angina despite unobstructed coronary arteries. CMR revealed severe asymmetric septal hypertrophy (D) with complete SAM in systole (E, yellow arrow) and turbulent LVOT flow due to LVOTO on rest. Case 3 (images G-I): 40-year-old man with severe exertional angina despite unobstructed coronary arteries. CMR revealed mid-apical HCM (G) with systolic mid-LV cavity obliteration with aneurysmal appearance of apical cap, albeit no apical aneurysm at this stage (H). Diffuse fibrosis in the hypertrophied apical segments contributed by severe coronary microvascular disease (I).

Risk stratification.

LGE is an important marker in risk stratification of SCD in HCM. Both LGE presence and extent have been evaluated. As a marker of dense replacement fibrosis, LGE correlates with histological evidence of raised collagen content in HCM myocardium[40]. LGE is present in 70-80% of HCM patients with varying extent (0-49% of imaged myocardium)[41], with typically mid-wall patchy distribution, affecting hypertrophied segments and RV insertion points (Figure 4). The relationship between LGE and the risk of death in HCM subjects is complex. In a prospective HCM study (n=220) with a mean follow up of 3 years, 20 have died and 2 had aborted SCD[42]. 90% of those who died had prior CMR evidence of LGE, while none of the "LGE-free" patients suffered cardiac death. Presence of any LGE on CMR was an independent predictor of death[42], however this notion was not maintained on multivariate analysis in another prospective HCM study[43].

As the extent of fibrosis correlates with the disease progression in HCM[41], the hypothesis that LGE extent (and not merely its presence) can predict the risk of adverse outcomes has been explored. In HCM, LGE extent (≥4 segments) is a predictor of spontaneous ventricular arrhythmias, independent of conventional risk factors for SCD[44]. In a prospective study by Ismail et al, 711 HCM subjects were followed for a median of 3.5 years, of whom 3.1% reached the primary end point (SCD or aborted SCD) and in this study LGE extent (but not its presence) was a significant predictor of the primary end point on univariable analysis, not maintained on multivariate analysis when adjusted for LVEF[45]. The SCD event rate was similar in a study by Chan et al[46], where 3% of 1293 HCM subjects suffered SCD during 3.3 years of follow up. In this study however, LGE extent was predictive of SCD events even after adjustment for relevant variables, with LGE ≥15% of LV mass being associated with a 2-fold increase in SCD in subjects considered to be at low risk based on conventional criteria[46]. Importantly, in a meta-analysis combining 2993 HCM patients of 5 eligible

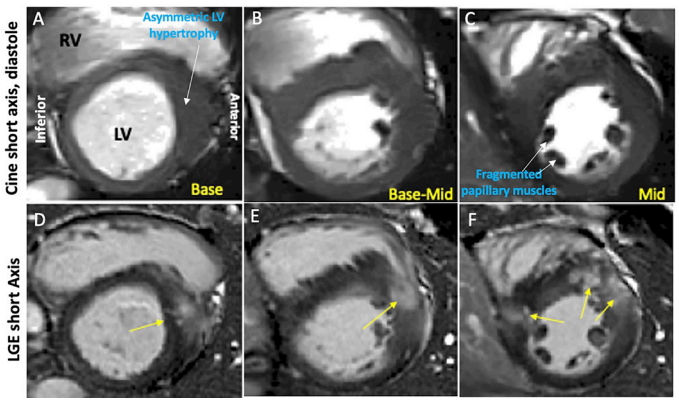

Figure 4. Myocardial fibrosis in HCM detected by LGE CMR. Cine CMR of ventricular short axis from base to mid (A-C) in a HCM subject described in Case 1 Figure 1, demonstrating asymmetric septal hypertrophy with "anticlockwise" involvement from anterior wall at the base, to the antero- and infero-septum at mid-apical LV levels. Myocardial fibrosis in HCM is shown (D-F) with arrowed areas of hyperintense signal signifying LGE with typical for HCM distribution: patchy, mid-wall, affecting hypertrophied LV regions and RV insertion points.

Phenotypic /clinical features	HCM	Hypertension induced LVH
History of hypertension	can be comorbid, usually well controlled	often poorly controlled
LVH pattern	commonly asymmetric	commonly concentric
LVH magnitude	15 mm and above	rarely exceeds 15 mm
LV mass index	⇔ or ⇧	⇧
Mitral SAM and LVOT obstruction	~ 60%	~ 5%
Papillary muscle abnormalities (hypertrophy, fragmentation, apical displacement, direct insertion into mitral valve leaflet)	+/-	-
Myocardial scar on LGE CMR	70-80%	20-25%
Response to antihypertensive therapy with tight BP control	BP control effect only	BP control and LVH regression

Table I. Phenotypic and clinical features differentiating hypertrophic cardiomyopathy and hypertension induced left ventricular hypertrophy.
LVH magnitude (maximal LV wall thickness)

studies, LGE extent was strongly associated with SCD risk even when adjusted for baseline characteristics[47]. In a recent 10-year follow up study, LGE extent of >5% of LV mass was shown to predict SCD risk in HCM subjects otherwise thought to be at low risk based on conventional risk criteria and SCD risk stratification tools[48]. The large HCMR study is underway which has sufficient power and duration of follow-up to determine the relation between LGE and mortality[49].

Differential Diagnosis

There are several phenocopies of HCM and CMR is invaluable for diagnostic differentiation directing appropriate and tailored therapy.

Anderson-Fabry Disease (AFD).

This is a rare X-linked inherited disorder characterised by glycosphingolipid deposition in tissues due to alpha-galactosidase deficiency. Cardiac involvement phenotypically resembles HCM, but typically with basal infero-lateral LGE[50] and low native T1 values[51], which discriminate AFD from other forms of LVH. This distinction is important as disease-specific management with enzyme replacement therapy in AFD is available[52].

Hypertensive heart disease.

LVH is an adaptive response to increased afterload in hypertension (HT-LVH). Differentiating HCM from HT-LVH is challenging. Some phenotypic and clinical markers help this process[53–56] Table I.

Cardiac Amyloidosis.

This is one of the most common causes of restrictive cardiomyopathy (RCM), but phenotypic overlap with HCM, renders inherent diagnostic challenges with over 30% of CA cases being misdiagnosed as HCM[57]. Crucially, CA has distinct pathophysiology and confers high mortality (~40% within 2 years in some subtypes)[58], hence the differentiation of CA from HCM is critically important to inform timely and disease-specific management. CA is characterised by tissue deposition of misfolded insoluble protein (amyloid), mainly due to either abnormal genetic variants (transthyretin, TTR amyloidosis) or plasma cell dyscrasia with monoclonal gammopathy (immunoglobulin light chain, AL amyloidosis)[1,59]. It is a multisystem disease, where cardiac involvement is typically manifested by small LV cavity with concentric mild-moderate LVH, commonly also right ventricular hypertrophy, thickening of atrioventricular valves and interatrial septum, pericardial and pleural effusions. Asymmetric LVH with or without LVOTO may be present in the early stages of the disease, leading to misdiagnosis as HCM[1,59]. There is often preserved LVEF, but impaired longitudinal and diastolic function with a restrictive filling pattern. Amyloid infiltration results in expansion of extracellular volume (with dominant involvement of subendocardium), resulting in a typical global circumferential subendocardial LGE pattern on CMR[60] Figure 5. In addition, a base-to-apical gradient of amyloid burden with relative apical sparing has been described[61,62]. In patients with congestive heart failure, LVH and a restrictive filling pattern, this typical LGE pattern has 80% sensitivity and 94% specificity for detecting biopsy-proven CA[63]. LGE extent can help differentiation between the AL and TTR forms of CA with a more extensive transmural LGE seen in the latter[64]. In addition, CA results in characteristically abnormal gadolinium kinetics with fast uptake of gadolinium by amyloid rich tissues and resultant dark blood pool within the first few minutes of gadolinium injection with difficulties in nulling the myocardium[60]. Furthermore, the degree of abnormality in gadolinium kinetics can predict outcome[65]. Native T1 values in CA are typically markedly elevated (differentiating from other causes of LVH such as aortic stenosis[65] and HCM[64]). ECV is also markedly elevated in CA and was shown to be an independent predictor of mortality in AL form[65].

Diabetic Cardiomyopathy.

This is characterised by myocardial structural and functional abnormalities in individuals with diabetes mellitus (DM) in the absence of abnormal loading conditions or coronary artery disease[66]. DM is an independent risk factor for development of

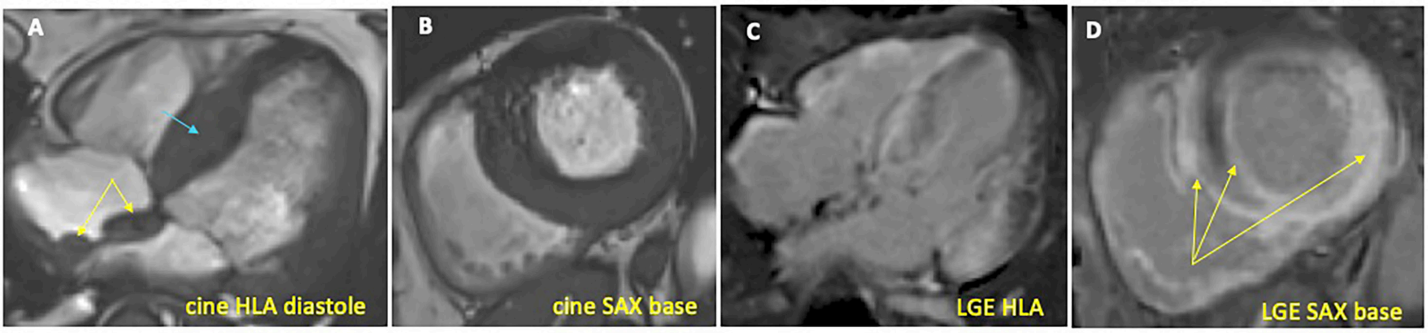

Figure 5. CMR in cardiac amyloidosis. Case 4 (images A-D): 65-year-old man with heart failure. CMR revealed severe predominantly concentric LVH (A, blue arrow), interatrial septal hypertrophy (A, yellow arrows) and diffuse circumferential subendocardial myocardial fibrosis pattern on LGE (C-D) with "zebra pattern" of LGE, involving subendocardial and subepicardial layers, but sparing the mid-myocardium in the septum (D, arrowed).

concentric LVH, which in turn is a predictor of cardiovascular mortality[67,68]. Clinical manifestations include: impaired LV longitudinal systolic and diastolic function, likely mediated by diffuse myocardial ffibrosis, which can be detected, quantified and thus monitored using CMR T1 mapping techniques[69,70]. Myocardial fibrosis however is thought to reflect the advanced stage of the disease, while cardiac steatosis (excessive intracellular accumulation of triglycerides) has been recently proposed as an underlying and potentially reversible mechanism for concentric LVH in type 2 DM[71].

Dilated Cardiomyopathy (DCM)

With relatively common prevalence (~1:400 of general population)[72], DCM is a common cause of heart failure and SCD and the most common indication for heart transplantation in young adults[73]. A genetic cause can be found in 10-40% of cases[72]. There is no cure for DCM and the mortality remains high despite available therapies (18-27% over 5 years)[74,75], but early diagnosis and prompt medical therapy modify the risk of adverse outcomes[76]. Thus, accurate phenotyping in subjects with suspected DCM has significant clinical ramifications (Figure 6).

Definition.

Dilated cardiomyopathy (DCM) is characterised by dilatation and systolic impairment of the left ventricle (with or without right ventricular involvement) not caused by abnormal loading conditions or coronary artery disease[1,77].

Phenotype

The defining features of DCM are LV chamber dilatation and LVEF reduction, thus accurate measurements are key to the diagnosis[1,77]. Whilst either echocardiography or CMR can be used for the initial diagnosis of DCM, CMR is a gold standard method for cardiac chambers volume quantification, with indexation for gender, age and body surface area and with its excellent reproducibility provides superior accuracy in the diagnosis and monitoring of response to therapy[7]. In addition, CMR can detect LV thrombi with superior accuracy compared to non-contrast echocardiography (87% vs 27%)[78]. This has direct implications for therapy and prevention of thromboembolism.

CMR provides highly reproducible and accurate quantification of LVEF, which is widely used as a descriptor of LV function and is a proven predictor of outcome in many cardiovascular diseases and heart failure[79]. Analysis of regional myocardial deformation (strain and strain rate) is emerging as a more accurate method of assessment of myocardial contractile function[80]. CMR deformation imaging techniques allow for such regional analysis[81]. Reduced longitudinal strain in DCM subjects by feature tracking CMR was shown to be a predictor of adverse outcomes independently of LVEF and

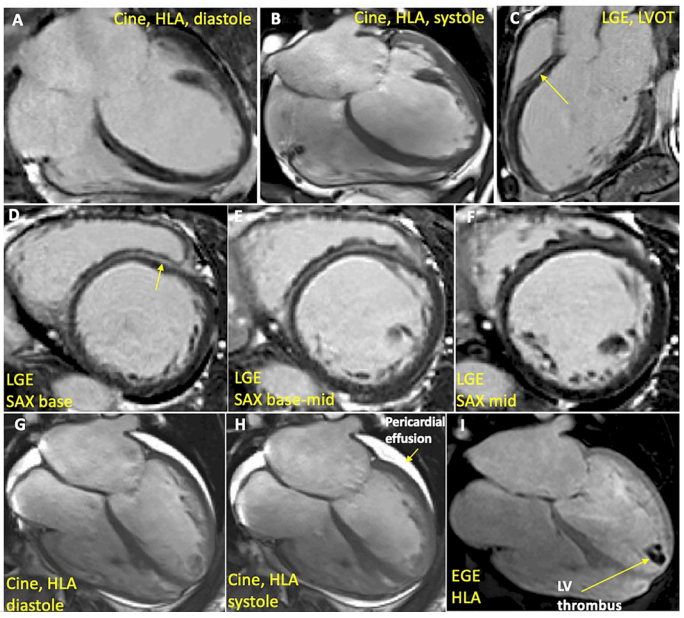

Figure 6. CMR in dilated cardiomyopathy. Case 5 (images A-F): 46-year-old man admitted with decompensated heart failure. CMR revealed severe biventricular dilatation and LVEF 16%, which combined with typical linear mid-wall fibrosis in the septum (C-F) is consistent with non-ischaemic DCM. Case 6 (images G-I): 35-year-old man admitted with cardiogenic shock. CMR revealed severe biventricular dilatation and LVEF 18%, There is also a pericardial effusion (H, arrowed) and a large LV apical thrombus noted on early gadolinium enhancement images (I, arrowed).

LGE extent[82]. Reduction of myocardial blood flow despite unobstructed coronaries is a recognised feature of DCM, reflective of disease severity rather than being a primary driver of disease pathophysiology[83].

Risk stratification

The LGE pattern in DCM has typically mid-wall and/or subepicardial distribution, affecting the interventricular septum where it is often linear, but also LV free wall and RV insertion points. It is present in 30-40% of DCM cases[84,85] and correlates with replacement fibrosis on histology[86]. In DCM, LGE presence and extent is associated with poor prognosis, including adverse LV remodelling, maintenance of re-entry ventricular arrhythmias[87] and is an independent predictor of SCD and all-cause mortality[74,85]. In a prospective study by Assomull et al[86], 101 DCM patients were followed up for a mean of 1.8 years. Mid-wall LGE on CMR was present in 35% of subjects. During follow-up, 17% of those with LGE vs 6% of those without LGE died. Mid-wall LGE was a significant predictor of combined end-point of all-cause mortality and cardiovascular hospitalisation (HR 3.4, p=0.01) and SCD or ventricular tachycardia (HR 5.2, p=0.03)[86]. In another prospective study of by Gulati et al[74], 472 of DCM patients were followed up for a median of 5.3 years. 26.8% of those with mid-wall LGE died vs 10.6% of those without LGE on CMR[74]. Both presence and extent of LGE on CMR were independently and incrementally associated with all-cause mortality; which were also independent predictors of other major adverse outcomes (cardiovascular mortality, cardiac transplantation, SCD and aborted SCD and the heart failure composite)[74]. In the meta-analysis, the annualised mortality in DCM with LGE was 4.7% vs 1.7% in those without LGE (p=0.01)[85]. The association between LGE extent and risk of adverse outcomes in DCM was shown to be non-linear in a large prospective study by Halliday et al[88], who followed 874 DCM patients for a median of 4.9 years. Even a small amount of non-ischaemic LGE conferred an increased risk of all-cause mortality (HR 1.81; 95% CI 1.3-2.5; p<0.001) independent of LVEF, age and gender[88]. Not only presence, but also LGE location informs risk stratification in DCM, with septal LGE associated with increased mortality, and combined septal and free wall LGE associated with increased risk of SCD[88].

Native T1 values and ECV are elevated in DCM when compared with controls[89]. Native T1 values were shown to independently predict all-cause mortality and a composite of heart failure hospitalisation and mortality in DCM[90].

Differential diagnosis

Both DCM and ischaemic damage are associated with adverse LV remodelling and dilatation, which if taken alone, can be indistinguishable in terms of underlying aetiology. In patients with new onset heart failure of unknown aetiology, LGE CMR is a robust non-invasive method enabling differentiation between ischaemic damage and DCM, with 97% diagnostic accuracy, which is non-inferior to invasive coronary angiogram[91]. The LGE pattern is typically subendocardial/transmural in myocardial infarction vs mid-wall/subepicardial in DCM[9] (Figure 7). The absence of the infarct LGE pattern does not completely rule out coronary artery disease as a cause of LV dilatation and dysfunction (as the phenomenon of global hibernation may occur[92], but this is uncommon). On the other hand, 13% of patients with impaired LV on echocardiography and angiographically unobstructed coronaries, are misdiagnosed as "non-ischaemic DCM"[84], while having evidence of an infarct LGE pattern on CMR, triggering re-evaluation of possible underlying aetiology, such as coronary plaque rupture and re-canalisation, coronary artery dissection or coronary thromboembolism. Each of these diagnoses mandates distinct management. The distinction between bystander vs attributable coronary artery disease is a matter of clinical judgement, taking into account coronary anatomy, myocardial tissue characterisation on CMR and clinical context.

Arrhythmogenic Right Ventricular Cardiomyopathy (ARVC)

Definition.

This is an arrhythmogenic heart muscle disorder not explained by ischaemic or abnormal loading factors[93]. It is relatively rare (population prevalence 1:1000-1:5000) but potentially fatal condition, with arrhythmias predominating the clinical picture (atrial and ventricular tachyarrhythmias and bradyarrhythmias). ARVC is an important cause of SCD in young adults and athletes[93]. The histopathological hallmarks of ARVC are cardiomyocyte atrophy and fibrofatty replacement. These changes are genetically determined, due to abnormal variants in the genes encoding the protein constituents of the cardiac desmosomal apparatus, intercalated discs and ion channels[93]. There is often a step-wise clinical progression with episodes of acute inflammatory infiltrates[94].

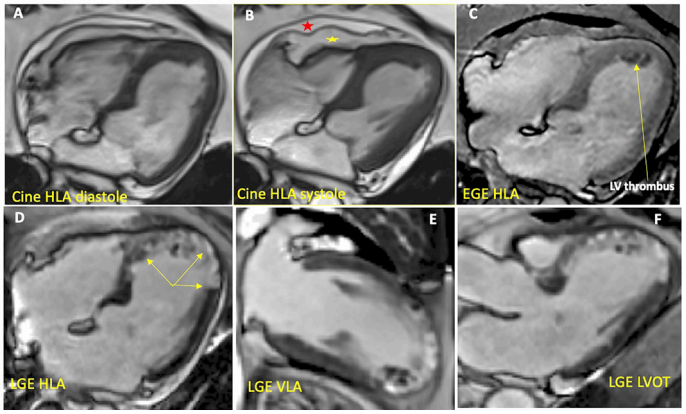

Figure 7. CMR in ischaemic cardiomyopathy. Case 7 (images A-F): 70-year-old woman with type 2 diabetes mellitus admitted with anterior ST elevation myocardial infarction and underwent primary percutaneous intervention to the left anterior descending (LAD) artery. CMR revealed dilated LV with severely impaired function (A-B). EGE images revealed LV apical thrombus (C, arrowed). Typical infarct LGE pattern (subendocardial to transmural) seen in the LAD distribution involves mid-apical antero-septum, anterior wall, all apical segments and apical cap (D-F). Pericardial effusion also noted (B, red star) and differentiated from excessive epicardial fat (B, yellow star).

Cardiovascular Magnetic Resonance in Cardiomyopathy

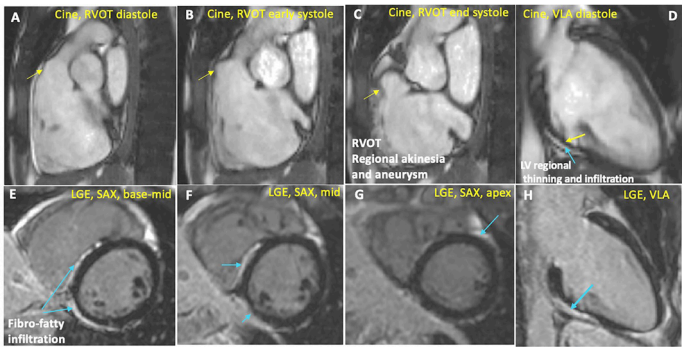

Figure 8. CMR in arrhythmogenic cardiomyopathy (biventricular involvement). Case 8 (images A-H): 40-year-old female admitted with palpitations, fever and raised serum cardiac troponin levels. Coronary angiogram revealed normal coronary arteries. Family history of suspected sudden death in the cousin age 28. CMR arranged as a follow up and revealed regional akinesia and aneurysm in the RVOT (A-C, yellow arrow), regional thinning and hypokinesia of basal-mid inferior LV wall (D, yellow arrow) with epicardial fibro-fatty replacement (D, blue arrow), extensive subepicardial fibro-fatty replacement of the RV side of interventricular septum, extending to inferior LV wall at base-mid LV levels, basal inferior RV wall and apical anterior wall (E-H, blue arrows).

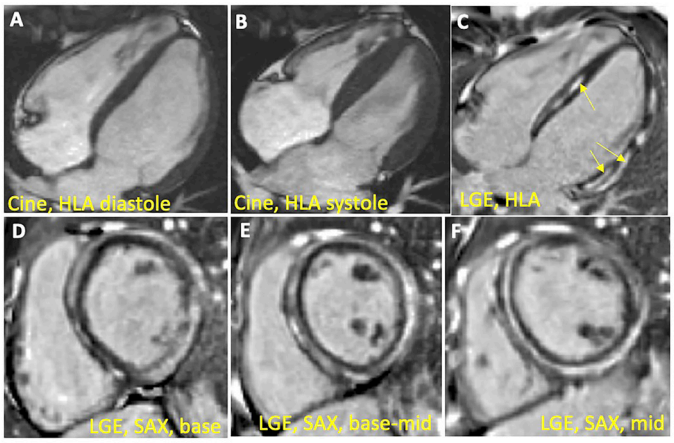

Figure 9. CMR in arrhythmogenic cardiomyopathy (LV-dominant form, ALVC). Case 9 (images A-F): 15-year-old male referred for screening following sudden death in his father with post-mortem histological evidence of fibrofatty myocardial infiltration consistent with ARVC. His Holter monitoring revealed increased ventricular ectopy burden and non-sustained ventricular tachycardia. CMR revealed normal biventricular size and function (A-B), however extensive circumferential mid-wall and epicardial myocardial fibrosis involving the majority of LV myocardium noted on LGE (C-F, yellow arrows) consistent with ALVC.

Phenotype.

The first description in 1980s referred to 24 cases with ventricular tachycardia associated with predominantly right ventricular pathology[95]. However, a range of phenotypic expressions are now recognised with RV (ARVC), LV-dominant (ALVC) or biventricular forms, hence the term "arrhythmogenic cardiomyopathy" (ACM) is increasingly being used[93]. The fibrofatty replacement typically progresses from epicardium through to the mid-myocardium to transmural involvement[94]. RV involvement in ACM is associated with RV dilatation, reduced RV ejection fraction (RVEF), wall thinning, microaneurysm formation and regional wall motion abnormalities (RWMA) with akinesia or dyskinesia[96] (Figure 8). LV involvement manifests with epicardial to mid-wall myocardial fibrofatty replacement, which is often circumferential[96] (Figure 9). Clinical diagnosis of ACM is challenging, and no single test is sufficient. The diagnosis is based on a scoring system proposed by the Task Force Criteria[96], combining clinical features (arrhythmias), ECG markers (T wave inversion and epsilon wave in the right precordial leads), family history, structural and functional abnormalities in RV and/or LV. CMR offers several advantages over other imaging modalities, as it can identify concurrent LV involvement and provides accurate and comprehensive characterisation of RV in terms of: indexed diastolic volumes, RVEF, RWMA, microaneurysm formation (cine), intramyocardial fat infiltration (spin echo fat suppressed technique) and fibrosis (LGE)[93,97]. Furthermore, more extensive LGE in ACM (typically ≥20% of LV mass) and mostly subepicardial pattern can differentiate ALVC and DCM[98].

Risk stratification.

LGE is typically difficult to detect in the thin RV wall and can be confounded by epicardial fat. In ALVC, LGE can be the first indicator of the disease process and confers the risk of adverse events, as malignant arrhythmias can occur despite relatively preserved LV function[93] (Figure 9). RV involvement in ALVC confers worse outcome[99].

Restrictive Cardiomyopathy (RCM)

Definition.

This is a heterogenous group of myocardial disorders and the least common of all cardiomyopathies. It is characterised by "ventricular stiffness" with restrictive ventricular physiology, defined by a precipitous rise in LV end diastolic pressure for only small increases in LV volume[1,59]. There are two main groups of causes: 1) myocardial infiltration or storage disorders (amyloidosis, glycogen storage, haemochromatosis, Anderson-Fabry disease, scleroderma, inflammatory or metastatic process); or 2) endomyocardial disorders with or without hypereosinophilia (endomyocardial fibrosis, fibroelastosis, pseudoxanthoma elasticum, carcinoid disease, toxicity or radiation induced)[1,59]. This review focuses on cardiac amyloidosis (described above) and iron overload (described below).

Phenotype.

RCM phenotype is usually that of biatrial enlargement, normal/reduced LV volumes, normal/near normal wall thickness and LVEF, but diastolic dysfunction and a restrictive filling pattern[1]. Echocardiography plays an important role in detecting and grading the latter and distinguishing RCM from constrictive pericarditis, both of which are characterised by a restrictive filling pattern[59]. CMR plays a unique role in differentiating between different aetiologies within RCM (using LGE, native and post contrast T1 and T2*mapping methods)[59]. CMR is

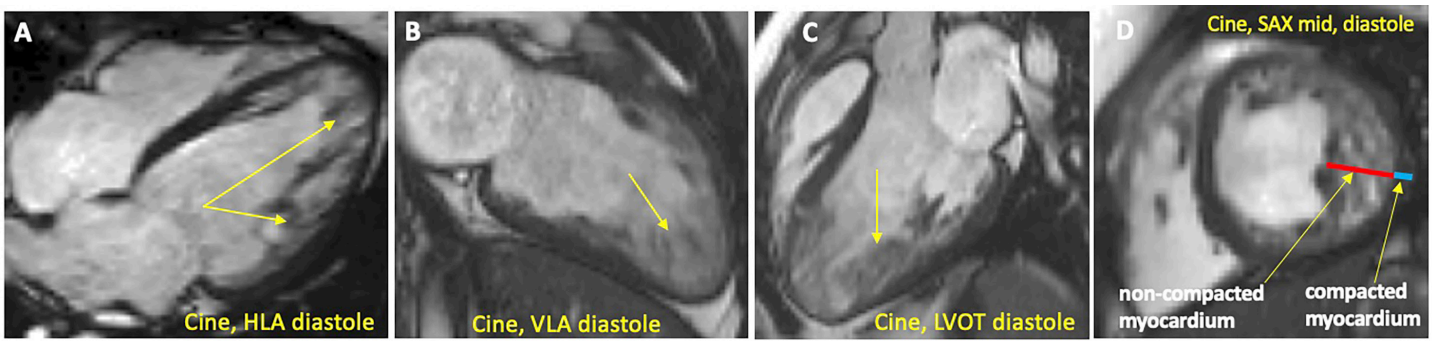

Figure 10. CMR in LV non compaction. Case 10 (images A-D): 16-year-old lady with recurrent atrial arrhythmias. CMR revealed mildly dilated LV with global hypokinesia, severely reduced LV function and excessive trabecular pattern in the mid-apical LV (A-C, yellow arrows). The ratio of non-compacted (red line) to compacted myocardium (blue line) in diastole in the inferolateral LV wall was 3.1 (D) meeting criteria for LVNC.

also helpful in non-invasive diagnosis of physiology pattern (using velocity encoded CMR) and differentiation from pericardial constriction (real time cine imaging to demonstrate interventricular interdependence and septal shift during respiration)[59].

Iron Overload (Siderotic) Cardiomyopathy.

Cardiac iron deposition in a form of haemosiderin occurs mainly as a result of regular blood transfusion due to chronic anaemia such as beta-thalassemia major, while being rare in hereditary haemochromatosis. It leads to a dilated and/or restrictive cardiomyopathy phenotype. Until 1999, heart failure was the primary cause of mortality in cardiac siderosis. Since then, T2* CMR imaging became available for cardiac iron content quantification[20], with normal myocardial T2* at 1.5T measured at midventricular septum is >20 ms, while lower values indicate cardiac siderosis. The discovery and application of T2* CMR revolutionised the management of cardiac siderosis, enabling early detection[20], risk stratification[100], direction and monitoring of cardiac iron chelation therapy (with deferiprone), all of which translated into a substantial 71% reduction in cardiac mortality in patients with thalassemia major[101].

Unclassified Cardiomyopathy

Left ventricular non compaction (LVNC).

LVNC is characterised by a mesh of myocardial trabeculations forming a non-compacted layer of LV myocardium (especially lateral and apical segments)[1,102]. The compacted epicardial layer is often relatively thin, may have ragged appearance and show regional dysfunction[1,102]. A genetic cause is found in 30-50% of patients with commonly sarcomere variants[103]. This is phenotypically and clinically heterogenous group of disorders with many forms described (LVNC, RVNC, biventricular, HCM form, RCM form, DCM form, or associated with congenital heart disease)[1]. LVNC is associated with heart failure, arrhythmias, systemic thromboembolism and sudden death[104]. The current diagnostic criteria mainly rely on distinction between non-compacted and compacted myocardial layers with the most commonly used criterion proposed by Petersen et al[102] (the ratio of non-compacted to compacted myocardium thickness at end diastole on CMR long axes views >2.3) (Figure 10). However, these criteria were shown to have poor specificity, found in 15% of individuals free from cardiovascular disease and hypertension[105], thus their use in isolation remains controversial. Furthermore, transient hypertrabeculation meeting these non-compaction criteria is observed in the context of altered loading conditions in a relatively high proportion of healthy individuals (athletes and pregnancy)[106,107], hence caution is required to avoid overdiagnosis. CMR based quantification of trabeculated myocardial mass (with the value of >20%) is proposed to have a better diagnostic accuracy[108]. Due to high spatial resolution, CMR is superior to echocardiography in the diagnosis of LVNC and can effectively differentiate LVNC from other cardiomyopathies, for example apical HCM[109]. In addition, CMR-based markers of myocardial deformation reflecting myocardial strain and twist were reported to be reduced in the affected segments of the LV and this correlated with the extent of non-compaction[110]. The LGE pattern in LVNC is similar to that in DCM and is associated with the poorer prognosis[111].

Role of CMR in the differential diagnosis of cardiomyopathies

One of the unique advantages of CMR is in the multiparametric assessment and ability to differentiate between various cardiomyopathy phenotypes as well as between different causes of a specific phenotype. Some of the key examples described below.

Myocarditis.

Myocardial inflammation can occur as a result of a range of injuries: viral, autoimmune, toxicity or ischaemia. Over 80% of presentations with presumed acute coronary syndrome yet unobstructed coronary arteries are due to acute myocarditis[112]. Endomyocardial biopsy remains a gold standard for the diagnosis confirmation, however it is not risk free[113]. In the context of acute myocarditis, myocardial oedema, inflammation and cardiomyocyte necrosis are the key manifestations detected by histology, which can be tracked by

Cardiovascular Magnetic Resonance in Cardiomyopathy

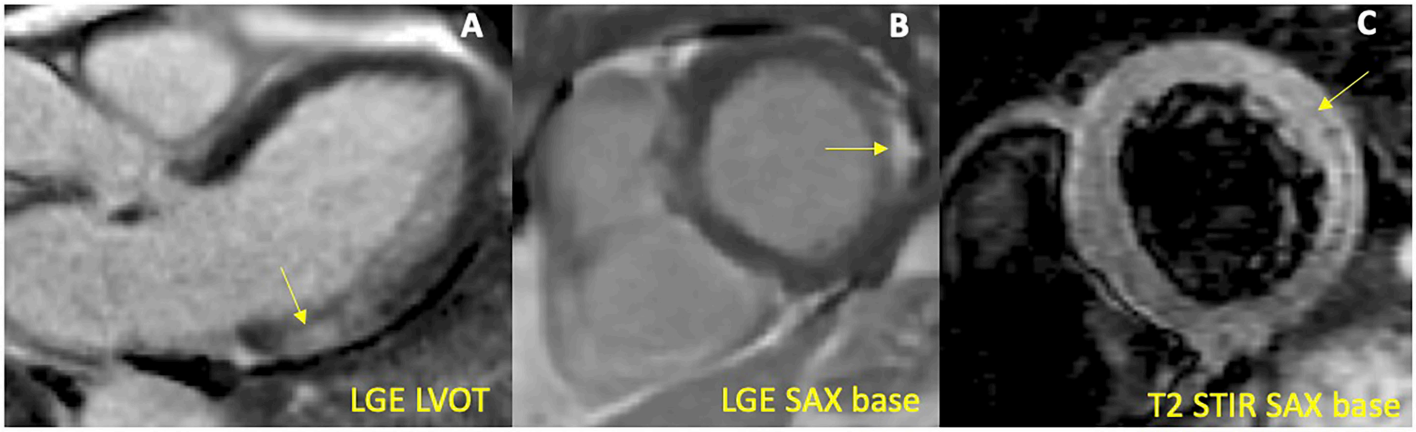

Figure 11. CMR in acute myocarditis. Case 11 (images A-C): 63-year-old man admitted with acute chest pain, ST segment elevation on ECG and elevated serum cardiac Troponin. Echocardiography revealed LV lateral wall hypokinesia. Coronary angiogram showed normal coronary arteries. CMR revealed normal biventricular size and function with basal lateral LV hypokinesia. CMR LGE images demonstrated subepicardial to mid-wall myocardial enhancement in the basal lateral wall (A-B, arrowed), which corresponded with the region of oedema/inflammation on the T2 STIR images (C, arrowed), consisted with acute myocarditis.

CMR (T2 and T1 mapping and LGE, summarised in the previous section). Elevated native T1 and T2 values, alongside mid-wall and/or subepicardial LGE pattern (especially in the lateral wall) are typically observed[114] (Figure 11). Furthermore, T2 relaxation time correlates closely with free water content in the myocardium, with the values raised in acute myocarditis and proposed to be the only CMR marker differentiating acute from convalescent myocarditis[114]. CMR diagnostic criteria for myocarditis ("Lake Louise criteria") were proposed and recently strengthened by quantitative parametric mapping methods[115], with native T1 (midventricular septal or global) suggested to improve diagnostic performance[116,117]. CMR parameters also inform risk stratification, with the presence and extent of septal LGE predicting downstream adverse LV remodelling and adverse outcomes[118].

Cardiac sarcoidosis (CS).

Sarcoidosis is a multi-system inflammatory disorder with a histological hallmark of noncaseating epithelioid tissue granulomas in the absence of other causes for granulomatous disease[119]. Cardiac involvement occurs in 25-50% and accounts for 25% of deaths in sarcoidosis, mainly due to heart failure and arrhythmic sudden death[120]. Early recognition is important as effective therapies exist[121]. Multimodality imaging, including CMR and 18F-fluorodeoxyglucose positron emission tomography, alongside multidisciplinary input are vital for the accurate diagnosis and management[122], emphasised in the recently updated Japanese Circulation Society guidelines[119]. Endomyocardial biopsy when positive is highly specific but has low sensitivity (<20%)[123]. CMR offers high diagnostic accuracy in CS, with high negative predictive value[124]. CS phenotypically can masquerade as DCM, HCM, RCM or ischaemic cardiomyopathy. Most commonly it is associated with LV dilatation, regional or global wall thinning and dysfunction. Regional abnormalities in LV wall thickness, with thinning (and possible aneurysm formation) or thickening are typical characteristics[119]. Active disease can be detected using T2-weighted images sensitive to oedema[125], which in combination with LGE detection of scar can discriminate between active and chronic CS[126] (Figure 12). LGE is present in over 70% of CS with a highly variable distribution pattern (mid-wall, subepicardial, subendocardial and/or transmural) in any of the LV and/or RV segments and even in papillary muscles, with the basal lateral segment being the most commonly involved[124]. A "shepherd's crook" LGE pattern with scar involving the basal antero-septum and RV anterior free wall is also typical, and associated with conduction abnormalities (Figure 12). LGE presence is a strong predictor of adverse outcome in CS, superior to LVEF[127,128]. In addition, LGE can guide biopsy sampling and monitor individual response to therapy[129].

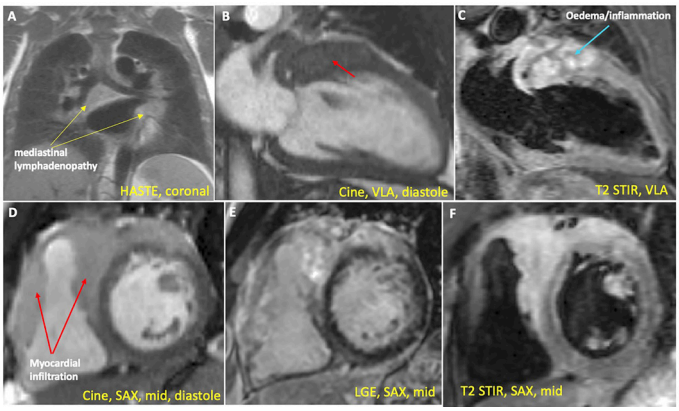

Figure 12. CMR in cardiac sarcoidosis. Case 12 (images A-F): 55-year-old man admitted with ventricular tachycardia. CMR revealed mediastinal lymphadenopathy (A, yellow arrows), regional thickening of anterior and anteroseptal base-mid LV wall and RV free wall (B and D, red arrows), which corresponded to regions of enhancement on LGE (E) and hyperintense signal on T2 STIR (C and F), consistent with acute inflammatory infiltrative process. Biopsy of lymph nodes revealed non-necrotising granulomata, confirming the diagnosis of sarcoidosis with cardiac and pulmonary involvement.

Phenotype	Phenotypic features	Cardiomyopathy	Athletic adaptation
DCM	Ventricular dilatation	++	+ (usually mild, balanced biventricular dilatation)
	Response to exercise stress test	LVEF ⇔ or ⇩ from baseline	LVEF ⇧ by >11% from baseline, peak exercise LVEF >63%
HCM / LVH	LV wall thickness	commonly >15 mm	commonly <15 mm
	E/E' on tissue Doppler echocardiography	⇔ or ⇧	⇔ or ⇩ and usually <12
	Native T1	⇔ or ⇧	⇩
	ECV	⇔ or ⇧	⇩
	Response to a period of detraining	⇔ unchanged LV wall thickness / mass	⇩ LV wall thickness ⇩ LV mass
ARVC	RV dilatation	++	+ (usually mild, balanced biventricular dilatation)
	RV regional wall motion abnormalities	++	-
Any	Myocardial fibrosis evidence on LGE CMR	+	-

Table II. Phenotypic features differentiating adverse remodelling in cardiomyopathy and physiologic athletic adaptation.

Athletic heart.

High intensity regular exercise activity aimed at endurance, performance and competition defines a highly trained athlete[130]. Athletic training has several physiological effects on cardiovascular system[131], including increased cardiac chamber volumes, increased LV wall thickness and LV mass. Ejection fraction of the LV and RV can be normal or reduced, but with improvement (>11%) on exercise echocardiography or CMR with peak LVEF >63%, with normal or even enhanced LV diastolic function[132,133]. Stroke volumes are typically >120mL. Myocardial fibrosis is usually pathologic, although septal and/or RV insertion point LGE in veteran athletes has been reported and remains of uncertain significance[134]. Phenotypic features favouring physiologic athletic adaptation vs pathologic remodelling in cardiomyopathy are summarised below (Table II)[131,135–139].

Novel CMR applications in cardiomyopathy: in vivo imaging of myocardial microstructure using diffusion tensor cardiovascular magnetic resonance (DT-CMR)

To date, DT-CMR is the only validated method for non-invasive in vivo evaluation of cardiac microstructure in humans[23–25]. It measures the signal loss generated by free water diffusion in the myocardium, allowing inferences to be made with respect to myocardial microarchitecture. In healthy myocardium, there is a primary helical arrangement of cardiomyocytes and a secondary laminar arrangement formed by aggregates of cardiomyocytes, termed sheetlets[140]. For every imaged myocardial voxel, DT-CMR can detect the predominant orientation of cardiomyocytes (helix angle) and sheetlets (secondary eigenvector angle, E2A) throughout the cardiac cycle, which has been validated against histology[141–143]. In health, sheetlets rotate from LV wall-parallel in diastole to LV wall-perpendicular orientation in systole (respectively colour coded as blue and red on examples below (Figure 13)[23,24]. Such sheetlet mobility is disturbed in cardiomyopathy, with sheetlets fixed in either a "systolic conformation" (HCM and cardiac amyloid) or a "diastolic conformation" (DCM)[141,144]. Furthermore, other non-contrast parameters obtained from DT-CMR (mean diffusivity and fractional anisotropy) can discriminate between HCM and its phenocopy cardiac amyloidosis[144], thus supporting diagnostic differentiation and the very different management strategies. DT-CMR provides unique insight into the mechanisms of impaired myocardial function in cardiomyopathy, not offered by other imaging modalities. These novel discoveries may inform future research into the disease-specific therapies, targeting the mechanisms implicated in the disease pathogenesis and revealed by DT-CMR.

CMR limitations

CMR may be limited by severe claustrophobia, significant irregular arrhythmias, inability to maintain periodic brief breath-holds (~10 seconds) and the presence of some implanted devices. The latter is being overcome by the increasing use of CMR conditional and CMR safe devices and carefully designed protocols with multidisciplinary infrastructure to allow safe scanning of these patients[145]. Use of GBCA is also restricted in certain scenarios, such as known hypersensitivity and in pregnant women, thus the need for GBCA use should be assessed individually to ensure safety[146]. Development of non-contrast techniques for myocardial tissue characterisation,

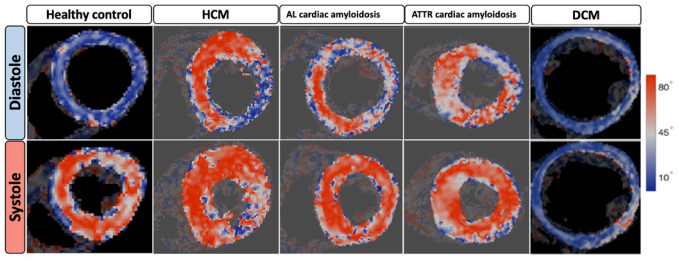

Figure 13. DT-CMR (diffusion tensor cardiovascular magnetic resonance) in cardiomyopathy. Colour coded maps represent the predominant orientation of absolute secondary eigenvector angle E2A (sheetlet orientation) for each imaged myocardial voxel of mid LV SAX slice in diastole and systole in a healthy control and subjects with cardiomyopathy (labelled). Normal change of sheetlet orientation (sheetlet mobility) from wall-parallel in diastole (coded as blue) to wall-perpendicular in systole (coded as red) seen in a healthy control. Sheetlet mobility is disturbed in cardiomyopathy subjects, with sheetlets fixed throughout the cardiac cycle in a "systolic conformation" (HCM and amyloidosis) or in a "diastolic conformation" (DCM)

such as DT-CMR, is an emerging field that may overcome these limitations.

Conclusion

Accurate phenotyping, differential diagnosis and risk stratification in cardiomyopathies is complex. CMR plays a central role in this process employing multiple techniques in one scan to accurately phenotype the condition and thus guide risk stratification and tailored treatment approaches.

Acknowledgements

This work was supported by a Programme Grant (RG/19/1/34160) from the British Heart Foundation.

Disclosures

DJ Pennell has received research funding from Siemens and speaker fees from Bayer and Chiesi.

Key abbreviations

ACM: arrhythmogenic cardiomyopathy
ALVC: arrhythmogenic left ventricular cardiomyopathy
AMVL: anterior mitral valve leaflet
ARVC: arrhythmogenic right ventricular cardiomyopathy
BP: blood pressure
CMR: cardiovascular magnetic resonance
DCM: dilated cardiomyopathy
ECG: electrocardiogram
ECV: extracellular volume
EGE: early gadolinium enhancement
EF: ejection fraction
GBCA: gadolinium-based contrast agent
HASTE: Half-Fourier Acquisition Single Short Turbo Spin Echo
HCM: hypertrophic cardiomyopathy
HLA: horizontal long axis
IVS: interventricular septum
LV: left ventricle
LVEF: left ventricular ejection fraction
LVNC: left ventricular non-compaction cardiomyopathy
LGE: late gadolinium enhancement
LVH: left ventricular hypertrophy
LVOT: left ventricular outflow tract
LVOTO: left ventricular outflow tract obstruction
RCM: restrictive cardiomyopathy
PMVL: posterior mitral valve leaflet
RV: right ventricle
RVOT: right ventricular outflow tract
RWMA: regional wall motion abnormalities
SAM: systolic anterior motion of mitral valve leaflet
SAX: short axis
SCD: sudden cardiac death
STIR: short tau inversion recovery
VLA: vertical long axis

References

1. Elliott P, Andersson B, Arbustini E, et al. Classification of the cardiomyopathies: A position statement from the european society of cardiology working group on myocardial and pericardial diseases. ***Eur Heart J***. 2008;29(2):270-276.
2. The Nobel Prize in Physics 1952. www.nobelprize.org/prizes/physics/1952/summary
3. Paul C. Lauterbur. www.nobelprize.org/prizes/medicine/2003/lauterbur/facts
4. Peter Mansfield. www.nobelprize.org/prizes/medicine/2003/mansfield/fact
5. Grothues F, Smith GC, Moon JCC, et al. Comparison of interstudy reproducibility of cardiovascular magnetic resonance with two-dimensional echocardiography in normal subjects and in patients with heart failure or left ventricular hypertrophy. ***Am J Cardiol***. 2002;90(1):29-34.
6. Bellenger N.G., Davies C.L., Francis J.M., Coats A.J.S., Pennell D.J. . Reduction in sample size for studies of remodeling in heart failure by the use of cardiovascular magnetic resonance. Published online 2000:271-278.
7. Maceira AM, Prasad SK, Khan M, Pennell DJ. Normalized left ventricular systolic and diastolic function by steady state free precession cardiovascular magnetic resonance. ***J Cardiovasc Magn Reson***. 2006;8(3):417-426.
8. Biglands JD, Radjenovic A, Ridgway JP. Cardiovascular magnetic resonance physics for clinicians: Part II. ***J Cardiovasc Magn Reson***. 2012;14(1):1-40.
9. Manning Warren J., Pennell Dudley ***J. . Cardiovascular Magnetic Resonance***. A Companion to Braunwald's Heart Disease.; 2019.
10. Goyal P, Weinsaft JW. Cardiovascular magnetic resonance imaging for assessment of cardiac thrombus. ***Methodist Debakey Cardiovasc J***. 2013;9(3):132-136.
11. Tomas G. Neilan, Otavio R. Coelho-Filho, Stephan B. Danik, Ravi V. Shah, John A. Dodson, Daniel J. Verdini, et al. CMR Quanti fi cation of Myocardial Scar Provides Additive Prognostic Information in Nonischemic Cardiomyopathy. ***JACC Cardiovasc Imaging***. 2013;6(9):944-954.
12. Flett AS, Hasleton J, Cook C, et al. Evaluation of techniques for the quantification of myocardial scar of differing etiology using cardiac magnetic resonance. ***JACC Cardiovasc Imaging***. 2011;4(2):150-156.
13. de Boer RA, De Keulenaer G, Bauersachs J, et al. Towards better definition, quantification and treatment of fibrosis in heart failure. A scientific roadmap by the Committee of Translational Research

of the Heart Failure Association (HFA) of the European Society of Cardiology. ***Eur J Heart Fail***. 2019;21(3):272-285.
14. Nguyen TP, Qu Z, Weiss JN. Cardiac fibrosis and arrhythmogenesis: The road to repair is paved with perils. ***J Mol Cell Cardiol.*** 2014;70:83-91.
15. Mewton N, Liu CY, Croisille P, Bluemke D, Lima JAC. Assessment of myocardial fibrosis with cardiovascular magnetic resonance. ***J Am Coll Cardiol***. 2011;57(8):891-903.
16. Haaf P, Garg P, Messroghli DR, Broadbent DA, Greenwood JP, Plein S. Cardiac T1 Mapping and Extracellular Volume (ECV) in clinical practice: A comprehensive review. ***J Cardiovasc Magn Reson***. 2016;18(1):1-12.
17. Flett AS, Hayward MP, Ashworth MT, et al. Equilibrium contrast cardiovascular magnetic resonance for the measurement of diffuse myocardial fibrosis: Preliminary validation in humans. ***Circulation***. 2010;122(2):138-144. doi:10.1161/CIRCULATIONAHA.109.930636
18. Friedrich MG, Sechtem U, Schulz-Menger J, et al. Cardiovascular Magnetic Resonance in Myocarditis: A JACC White Paper. ***J Am Coll Cardiol.*** 2009;53(17):1475-1487.
19. Ridgway JP. Cardiovascular magnetic resonance physics for clinicians: Part i. ***J Cardiovasc Magn Reson***. 2010;12(1):71. http://www.jcmr-online.com/content/12/1/71
20. Anderson LJ, Holden S, Davis B, et al. Cardiovascular T2-star (T2*) magnetic resonance for the early diagnosis of myocardial iron overload. ***Eur Heart J***. 2001;22(23):2171-2179.
21. Carpenter JP, He T, Kirk P, et al. On T2* magnetic resonance and cardiac iron. ***Circulation***. 2011;123(14):1519-1528.
22. Edelman RR, Gaa J, Wedeen VJ, et al. In vivo measurement of water diffusion in the human heart. ***Magn Reson Med***. 1994;32(3):423-428.
23. Nielles-Vallespin S, Scott A, Ferreira P, Khalique Z, Pennell D, Firmin D. Cardiac Diffusion: Technique and Practical Applications. ***J Magn Reson Imaging***. Published online 2019.
24. Khalique Z, Ferreira PF, Scott AD, Nielles-Vallespin S, Firmin DN, Pennell DJ. Diffusion Tensor Cardiovascular Magnetic Resonance Imaging: A Clinical Perspective. ***JACC Cardiovasc Imaging***. Published online 2019.
25. Mekkaoui C, Reese TG, Jackowski MP, Bhat H, Sosnovik DE. Diffusion MRI in the heart. ***NMR Biomed***. 2017;30(3):1-2.
26. Yuchi Han, Timo Liimatainen, Robert C. Gorman, Walter R. T. Witschey,. Assessing Myocardial Disease Using T1ρ MRI. Curr ***Cardiovasc Imaging Rep***. 2014;7(2):1-17.
27. Wang L, Yuan J, Zhang SJ, et al. Myocardial T1rho mapping of patients with end-stage renal disease and its comparison with T1 mapping and T2 mapping: A feasibility and reproducibility study. ***J Magn Reson Imaging***. 2016;44(3):723-731. doi:10.1002/jmri.25188
28. O'Mahony C, Jichi F, Pavlou M, et al. A novel clinical risk prediction model for sudden cardiac death in hypertrophic cardiomyopathy (HCM Risk-SCD). ***Eur Heart J.*** 2014;35(30):2010-2020.
29. Hershberger RE, Givertz MM, Ho CY, et al. Genetic Evaluation of Cardiomyopathy: A Heart Failure Society of America Practice Guideline. ***J Card Fail***. 2018;24(5):281-302.
30. Elliott, Perry M., Zamorano JL, Anastasakis A, Borger MA, et al. 2014 ESC Guidelines on diagnosis and management of hypertrophic cardiomyopathy. ***Eur Heart J***. 2014;35(39):2733-2779.
31. Gersh BJ, Maron BJ, Bonow RO, et al. 2011 ACCF/AHA Guidelines for the Diagnosis and Treatment of Hypertrophic Cardiomyopathy. ***Circulation***. 2011;124(24):2761-2796.
32. Hughes SE. The pathology of hypertrophic cardiomyopathy. ***Histopathology***. 2004;44(5):412-427.
33. Imran S. Syed, Steve R. Ommen, Jerome F. Breen, and A. Jamil Tajik, . Hypertrophic Cardiomyopathy : Identification of Morphological Subtypes by Echocardiography and Cardiac Magnetic Resonance Imaging. ***JACC Cardiovasc Imaging***. 2008;1(3):377-379.
34. Rickers C, Wilke NM, Jerosch-Herold M, et al. Utility of cardiac magnetic resonance imaging in the diagnosis of hypertrophic cardiomyopathy. ***Circulation***. 2005;112(6):855-861.
35. Moon JCC, Fisher NG, McKenna WJ, Pennell DJ. Detection of apical hypertrophic cardiomyopathy by cardiovascular magnetic resonance in patients with non-diagnostic echocardiography. ***Heart***. 2004;90(6):645-649.
36. Vigneault DM, Yang E, Jensen PJ, et al. Left Ventricular Strain Is Abnormal in Preclinical and Overt Hypertrophic Cardiomyopathy: Cardiac MR Feature Tracking. ***Radiology***. 2019;290(3):640-648.
37. Hinojar R, Fernández-Golfín C, González-Gómez A, et al. Prognostic implications of global myocardial mechanics in hypertrophic cardiomyopathy by cardiovascular magnetic resonance feature tracking. Relations to left ventricular hypertrophy and fibrosis. ***Int J Cardiol***. 2017;249:467-472.
38. Ismail TF, Hsu L-Y, Greve AM, et al. Coronary microvascular ischemia in hypertrophic cardiomyopathy - a pixel-wise quantitative cardiovascular magnetic resonance perfusion study. ***J Cardiovasc Magn Reson***. 2014;16(1):1-10.
39. Maron MS, Olivotto I, Maron BJ, et al. The Case for Myocardial Ischemia in Hypertrophic Cardiomyopathy. ***J Am Coll Cardiol***. 2009;54(9):866-875.
40. Moon JCC, Reed E, Sheppard MN, et al. The histologic basis of late gadolinium enhancement cardiovascular magnetic resonance in hypertrophic cardiomyopathy. ***J Am Coll Cardiol***. 2004;43(12):2260-2264.
41. Moon JCC, McKenna WJ, McCrohon JA, Elliott PM, Smith GC, Pennell DJ. Toward clinical risk assessment in hypertrophic cardiomyopathy with gadolinium cardiovascular magnetic resonance. ***J Am Coll Cardiol***. 2003;41(9):1561-1567.
42. Bruder O, Wagner A, Jensen CJ, et al. Myocardial scar visualized by cardiovascular magnetic resonance imaging predicts major adverse events in patients with hypertrophic cardiomyopathy. ***J Am Coll Cardiol.*** 2010;56(11):875-887.
43. O'Hanlon R, Grasso A, Roughton M, et al. Prognostic significance of myocardial fibrosis in hypertrophic cardiomyopathy. ***J Am Coll Cardiol***. 2010;56(11):867-874.
44. Park YJ, Park SJ, Kim EK, et al. Semi-quantitative versus quantitative assessments of late gadolinium enhancement extent for predicting spontaneous ventricular tachyarrhythmia events in patients with hypertrophic cardiomyopathy. ***Sci Rep***. 2020;10(1):1-8.
45. Ismail TF, Jabbour A, Gulati A, et al. Role of late gadolinium enhancement cardiovascular magnetic resonance in the risk stratification of hypertrophic cardiomyopathy. ***Heart***. 2014;100(23):1851-1858.
46. Chan RH, Maron BJ, Olivotto I, et al. Prognostic value of quantitative contrast-enhanced cardiovascular magnetic resonance for the evaluation of sudden death risk in patients with hypertrophic cardiomyopathy. ***Circulation***. 2014;130(6):484-495.
47. Weng Z, Yao J, Chan RH, et al. Prognostic Value of LGE-CMR in HCM. ***JACC Cardiovasc Imaging.*** 2016;9(12):1392-1402.
48. Greulich S, Seitz A, Herter D, et al. Long-term risk of sudden cardiac death in hypertrophic cardiomyopathy: a cardiac magnetic resonance outcome study. ***Eur Hear J - Cardiovasc Imaging***. Published online 2021:1-10.
49. Neubauer S, Kolm P, Ho CY, et al. Distinct Subgroups in Hypertrophic Cardiomyopathy in the NHLBI HCM Registry. ***J Am Coll Cardiol***. 2019;74(19):2333-2345.
50. De Cobelli F, Esposito A, Belloni E, et al. Delayed-enhanced cardiac MRI for differentiation of fabry's disease from symmetric hypertrophic cardiomyopathy. ***Am J Roentgenol***. 2009;192(3):97-102.
51. Sado DM, White SK, Piechnik SK, et al. Identification and assessment of anderson-fabry disease by cardiovascular magnetic resonance noncontrast myocardial T1 mapping. ***Circ Cardiovasc Imaging***. 2013;6(3):392-398.
52. Moon JCC, Sachdev B, Elkington AG, et al. Gadolinium enhanced cardiovascular magnetic resonance in Anderson-Fabry disease: Evidence for a disease specific abnormality of the myocardial interstitium. ***Eur Heart J***. 2003;24(23):2151-2155.
53. Mavrogeni S, Katsi V, Vartela V, et al. The emerging role of Cardiovascular Magnetic Resonance in the evaluation of hypertensive heart disease. ***BMC Cardiovasc Disord.*** 2017;17(1):1-10.
54. Hinojar R, Varma N, Child N, et al. T1 Mapping in Discrimination

of Hypertrophic Phenotypes: Hypertensive Heart Disease and Hypertrophic Cardiomyopathy: Findings from the International T1 Multicenter Cardiovascular Magnetic Resonance Study. ***Circ Cardiovasc Imaging***. 2015;8(12):1-9.
55. Devereux RB, Dahlöf B, Gerdts E, et al. Regression of hypertensive left ventricular hypertrophy by Losartan compared with atenolol: The Losartan Intervention for Endpoint Reduction in Hypertension (LIFE) trial. ***Circulation***. 2004;110(11):1456-1462.
56. Argulian E, Messerli FH, Aziz EF, et al. Antihypertensive therapy in hypertrophic cardiomyopathy. ***Am J Cardiol.*** 2013;111(7):1040-1045.
57. Siddiqi OK, Ruberg FL. Challenging the myths of cardiac amyloidosis. ***Eur Heart J***. 2017;38(24):1909-1912.
58. Rapezzi C, Merlini G, Quarta CC, et al. Systemic cardiac amyloidoses: Disease profiles and clinical courses of the 3 main types. ***Circulation***. 2009;120(13):1203-1212.
59. Habib G, Bucciarelli-Ducci C, Caforio ALP, et al. Multimodality Imaging in Restrictive Cardiomyopathies: An EACVI expert consensus document In collaboration with the "Working Group on myocardial and pericardial diseases" of the European Society of Cardiology Endorsed by The Indian Academy of Echocardiogr. ***Eur Heart J Cardiovasc Imaging***. 2017;18(10):1090-1091. doi:10.1093/ehjci/jex034
60. Maceira AM, Joshi J, Prasad SK, et al. Cardiovascular magnetic resonance in cardiac amyloidosis. ***Circulation***. 2005;111(2):186-193.
61. Phelan D, Collier P, Thavendiranathan P, et al. Relative apical sparing of longitudinal strain using two-dimensional speckle-tracking echocardiography is both sensitive and specific for the diagnosis of cardiac amyloidosis. ***Heart***. 2012;98(19):1442-1448.
62. Oda S, Kawano Y, Okuno Y, et al. Base-to-apex gradient pattern of cardiac impairment identified on myocardial T1 mapping in cardiac amyloidosis. ***Radiol Case Reports***. 2019;14(1):72-74.
63. Vogelsberg H, Mahrholdt H, Deluigi CC, et al. Cardiovascular Magnetic Resonance in Clinically Suspected Cardiac Amyloidosis. Noninvasive Imaging Compared to Endomyocardial Biopsy. ***J Am Coll Cardiol.*** 2008;51(10):1022-1030.
64. Fontana M, Banypersad SM, Treibel TA, et al. Native T1 mapping in transthyretin amyloidosis. ***JACC Cardiovasc Imaging***. 2014;7(2):157-165.
65. Maceira AM, Prasad SK, Hawkins PN, Roughton M, Pennell DJ. Cardiovascular magnetic resonance and prognosis in cardiac amyloidosis. ***J Cardiovasc Magn Reson***. 2008;10(1):1-11.
66. Jia G, Hill MA, Sowers JR. Diabetic cardiomyopathy: An update of mechanisms contributing to this clinical entity. ***Circ Res***. 2018;122(4):624-638.
67. Devereux RB, Roman MJ, Paranicas M, et al. Impact of diabetes on cardiac structure and function: The Strong Heart Study. ***Circulation***. 2000;101(19):2271-2276.
68. Bluemke DA, Kronmal RA, Lima JAC, et al. The Relationship of Left Ventricular Mass and Geometry to Incident Cardiovascular Events. The MESA (Multi-Ethnic Study of Atherosclerosis) Study. ***J Am Coll Cardiol***. 2008;52(25):2148-2155.
69. Ng ACT, Auger D, Delgado V, et al. Association between diffuse myocardial fibrosis by cardiac magnetic resonance contrast-enhanced T1 mapping and subclinical myocardial dysfunction in diabetic patients a pilot study. ***Circ Cardiovasc Imaging***. 2012;5(1):51-59.
70. Jellis C, Wright J, Kennedy D, et al. Association of imaging markers of myocardial fibrosis with metabolic and functional disturbances in early diabetic cardiomyopathy. ***Circ Cardiovasc Imaging***. 2011;4(6):693-702.
71. Eylem Levelt, Masliza Mahmod, Stefan K. Piechnik, Rina Ariga, Jane M. Francis, Christopher T. Rodgers, et al. Relationship between Left Ventricular Structural and Metabolic Remodelling in Type 2 Diabetes Mellitus. ***Diabetes***. 2016;65(1):44-52.
72. Hershberger RE, Hedges DJ, Morales A. Dilated cardiomyopathy: The complexity of a diverse genetic architecture. ***Nat Rev Cardiol***. 2013;10(9):531-547.
73. Stehlik J, Edwards LB, Kucheryavaya AY, et al. The registry of the international society for heart and lung transplantation: Twenty-eighth adult heart transplant report-2011. ***J Hear Lung Transplant***. 2011;30(10):1078-1094.
74. Gulati A, Jabbour A, Ismail TF, et al. Association of fibrosis with mortality and sudden cardiac death in patients with nonischemic dilated cardiomyopathy. ***JAMA - J Am Med Assoc***. 2013;309(9):896-908.
75. Halliday BP, Gulati A, Ali A, et al. Association between midwall late gadolinium enhancement and sudden cardiac death in patients with dilated cardiomyopathy and mild and moderate left ventricular systolic dysfunction. ***Circulation***. 2017;135(22):2106-2115.
76. Merlo M, Pivetta A, Pinamonti B, et al. Long-term prognostic impact of therapeutic strategies in patients with idiopathic dilated cardiomyopathy: changing mortality over the last 30 years. ***Eur J Heart Fail***. 2014;16(3):317-324.
77. Pinto YM, Elliott PM, Arbustini E, et al. Proposal for a revised definition of dilated cardiomyopathy, hypokinetic non-dilated cardiomyopathy, and its implications for clinical practice: A position statement of the ESC working group on myocardial and pericardial diseases. ***Eur Heart J.*** 2016;37(23):1850-1858.
78. Srichai MB, Junor C, Rodriguez LL, et al. Clinical, imaging, and pathological characteristics of left ventricular thrombus: A comparison of contrast-enhanced magnetic resonance imaging, transthoracic echocardiography, and transesophageal echocardiography with surgical or pathological validation. ***Am Heart J***. 2006;152(1):75-84.
79. Solomon SD, Anavekar N, Skali H, et al. Influence of ejection fraction on cardiovascular outcomes in a broad spectrum of heart failure patients. ***Circulation***. 2005;112(24):3738-3744.
80. Pryds K, Larsen AH, Hansen MS, et al. Myocardial strain assessed by feature tracking cardiac magnetic resonance in patients with a variety of cardiovascular diseases - A comparison with echocardiography. ***Sci Rep***. 2019;9(1):11296.
81. Amzulescu MS, De Craene M, Langet H, et al. Myocardial strain imaging: Review of general principles, validation, and sources of discrepancies. ***Eur Heart J Cardiovasc Imaging***. 2019;20(6):605-619.
82. Buss SJ, Breuninger K, Lehrke S, et al. Assessment of myocardial deformation with Cardiac magnetic resonance strain imaging improves risk stratification in patients with dilated cardiomyopathy. ***Eur Heart J Cardiovasc Imaging***. 2015;16(3):307-315.
83. Dass S, Holloway CJ, Cochlin LE, et al. No Evidence of Myocardial Oxygen Deprivation in Nonischemic Heart Failure. ***Circ Hear Fail***. 2015;8(6):1088-1093.
84. McCrohon JA, Moon JCC, Prasad SK, et al. Differentiation of heart failure related to dilated cardiomyopathy and coronary artery disease using gadolinium-enhanced cardiovascular magnetic resonance. ***Circulation***. 2003;108(1):54-59.
85. Kuruvilla S, Adenaw N, Katwal AB, Lipinski MJ, Kramer CM, Salerno M. Late gadolinium enhancement on cardiac magnetic resonance predicts adverse cardiovascular outcomes in nonischemic cardiomyopathy: A systematic review and meta-analysis. ***Circ Cardiovasc Imaging***. 2014;7(2):250-257.
86. Assomull RG, Prasad SK, Lyne J, et al. Cardiovascular Magnetic Resonance, Fibrosis, and Prognosis in Dilated Cardiomyopathy. ***J Am Coll Cardiol***. 2006;48(10):1977-1985.
87. Henry H Hsia, Francis E Marchlinski. Electrophysiology studies in patients with dilated cardiomyopathies. ***Card Electrophysiol Rev***. 2002;6(4):472–481.
88. Halliday BP, Baksi AJ, Gulati A, et al. Outcome in Dilated Cardiomyopathy Related to the Extent, Location, and Pattern of Late Gadolinium Enhancement. ***JACC Cardiovasc Imaging***. 2019;12(8P2):1645-1655.
89. Puntmann VO, Voigt T, Chen Z, et al. Native T1 mapping in differentiation of normal myocardium from diffuse disease in hypertrophic and dilated cardiomyopathy. ***JACC Cardiovasc Imaging***. 2013;6(4):475-484.
90. Puntmann VO, Carr-White G, Jabbour A, et al. T1-Mapping and Outcome in Nonischemic Cardiomyopathy All-Cause Mortality and Heart Failure. ***JACC Cardiovasc Imaging***. 2016;9(1):40-50.

91. Assomull RG, Shakespeare C, Kalra PR, et al. Role of cardiovascular magnetic resonance as a gatekeeper to invasive coronary angiography in patients presenting with heart failure of unknown etiology. ***Circulation***. 2011;124(12):1351-1360.
92. Kloner RA. Stunned and Hibernating Myocardium: Where Are We Nearly 4 Decades Later? ***J Am Heart Assoc***. 2020;9(3):1-11.
93. Towbin JA, McKenna WJ, Abrams DJ, et al. 2019 HRS expert consensus statement on evaluation, risk stratification, and management of arrhythmogenic cardiomyopathy. ***Hear Rhythm***. 2019;16(11):e301-e372.
94. Corrado D, Basso C, Thiene G, et al. Spectrum of clinicopathologic manifestations of arrhythmogenic right ventricular cardiomyopathy/dysplasia: A multicenter study. ***J Am Coll Cardiol***. 1997;30(6):1512-1520.
95. Marcus FI, Fontaine GH, Guiraudon G, et al. Right ventricular dysplasia: A report of 24 adult cases. ***Ann Noninvasive Electrocardiol***. 1999;4(1):97-111.
96. Marcus FI, McKenna WJ, Sherrill D, et al. Diagnosis of arrhythmogenic right ventricular cardiomyopathy/Dysplasia: Proposed modification of the task force criteria. ***Circulation***. 2010;121(13):1533-1541.
97. Corrado D, Van Tintelen PJ, McKenna WJ, et al. Arrhythmogenic right ventricular cardiomyopathy: Evaluation of the current diagnostic criteria and differential diagnosis. ***Eur Heart J***. 2020;41(14):1414-1427b. doi:10.1093/eurheartj/ehz669
98. Cipriani A, Bauce B, De Lazzari M, et al. Arrhythmogenic Right Ventricular Cardiomyopathy: Characterization of Left Ventricular Phenotype and Differential Diagnosis With Dilated Cardiomyopathy. ***J Am Heart Assoc***. 2020;9(5):e014628.
99. He J, Xu J, Li G, et al. Arrhythmogenic Left Ventricular Cardiomyopathy: A Clinical and CMR Study. ***Sci Rep***. 2020;10(1):1-12.
100. Kirk P, Roughton M, Porter JB, et al. Cardiac T2* magnetic resonance for prediction of cardiac complications in Thalassemia Major. ***Circulation***. 2009;120(20):1961-1968.
101. Modell B, Khan M, Darlison M, Westwood MA, Ingram D, Pennell DJ. Improved survival of thalassaemia major in the UK and relation to T2* cardiovascular magnetic resonance. ***J Cardiovasc Magn Reson***. 2008;10(1):1-8. doi:10.1186/1532-429X-10-42
102. Petersen SE, Selvanayagam JB, Wiesmann F, et al. Left ventricular non-compaction: Insights from cardiovascular magnetic resonance imaging. ***J Am Coll Cardiol***. 2005;46(1):101-105.
103. Ichida F, Hamamichi Y, Miyawaki T, et al. Clinical features of isolated noncompaction of the ventricular myocardium. ***J Am Coll Cardiol***. 1999;34(1):233-240.
104. Thavendiranathan P, Dahiya A, Phelan D, Desai MY, Wilson Tang WH. Isolated left ventricular non-compaction controversies in diagnostic criteria, adverse outcomes and management. ***Heart***. 2013;99(10):681-689.
105. Jonathan R. Weir-McCall, Phey Ming Yeap, Carla Papagiorcopulo, Kerrie Fitzgerald, Stephen J. Gandy, Matthew Lambert, et al. Left ventricular noncompaction. ***Clin Cardiogenetics*** Second Ed. 2016;68(20):113-135.
106. Gati S, Papadakis M, Papamichael ND, et al. Reversible de novo left ventricular trabeculations in pregnant women: Implications for the diagnosis of left ventricular noncompaction in low-risk populations. ***Circulation***. 2014;130(6):475-483.
107. Peritz DC, Vaughn A, Ciocca M, Chung EH. Hypertrabeculation vs left ventricular noncompaction on echocardiogram: A reason to restrict athletic participation? J***AMA Intern Med***. 2014;174(8):1379-1382.
108. Jacquier A, Thuny F, Jop B, et al. Measurement of trabeculated left ventricular mass using cardiac magnetic resonance imaging in the diagnosis of left ventricular non-compaction. ***Eur Heart J***. 2010;31(9):1098-1104.
109. Thuny F, Jacquier A, Jop B, et al. Assessment of left ventricular non-compaction in adults: Side-by-side comparison of cardiac magnetic resonance imaging with echocardiography. ***Arch Cardiovasc Dis***. 2010;103(3):150-159.
110. Gastl M, Gotschy A, Polacin M, et al. Determinants of myocardial function characterized by CMR-derived strain parameters in left ventricular non-compaction cardiomyopathy. ***Sci Rep***. 2019;9(1):1-10.
111. Grigoratos C, Barison A, Ivanov A, et al. Meta-Analysis of the Prognostic Role of Late Gadolinium Enhancement and Global Systolic Impairment in Left Ventricular Noncompaction. ***JACC Cardiovasc Imaging***. 2019;12(11P1):2141-2151.
112. Monney PA, Sekhri N, Burchell T, et al. Acute myocarditis presenting as acute coronary syndrome: Role of early cardiac magnetic resonance in its diagnosis. ***Heart***. 2011;97(16):1312-1318.
113. Caforio ALP, Pankuweit S, Arbustini E, et al. Current state of knowledge on aetiology, diagnosis, management, and therapy of myocarditis: A position statement of the European Society of Cardiology Working Group on Myocardial and Pericardial Diseases. ***Eur Heart J***. 2013;34(33):2636-2648.
114. Bohnen S, Radunski UK, Lund GK, et al. Performance of T1 and T2 Mapping Cardiovascular Magnetic Resonance to Detect Active Myocarditis in Patients with Recent-Onset Heart Failure. ***Circ Cardiovasc Imaging***. 2015;8(6):1-7.
115. Ferreira VM, Schulz-Menger J, Holmvang G, et al. Cardiovascular Magnetic Resonance in Nonischemic Myocardial Inflammation: Expert Recommendations. ***J Am Coll Cardiol***. 2018;72(24):3158-3176.
116. Lurz P, Luecke C, Eitel I, et al. Comprehensive Cardiac Magnetic Resonance Imaging in Patients with Suspected Myocarditis the MyoRacer-Trial. ***J Am Coll Cardiol***. 2016;67(15):1800-1811.
117. Dabir D, Vollbrecht TM, Luetkens JA, et al. Multiparametric cardiovascular magnetic resonance imaging in acute myocarditis: a comparison of different measurement approaches. ***J Cardiovasc Magn Reson***. 2019;21(1):1-11.
118. Greulich S, Seitz A, Müller KAL, et al. Predictors of Mortality in Patients With Biopsy-Proven Viral Myocarditis: 10-Year Outcome Data. ***J Am Heart Assoc***. 2020;9(16):e015351.
119. Terasaki F, Azuma A, Anzai T, et al. JCS 2016 guideline on diagnosis and treatment of cardiac sarcoidosis. ***Circ J***. 2019;83(11):2329-2388.
120. Doughan AR, Williams BR. Cardiac sarcoidosis. ***Heart***. 2006;92(2):282-288.
121. Yazaki Y, Isobe M, Hiroe M, et al. Prognostic determinants of long-term survival in Japanese patients with cardiac sarcoidosis treated with prednisone. ***Am J Cardiol***. 2001;88(9):1006-1010.
122. Slart RHJA, Glaudemans AWJM, Lancellotti P, et al. A joint procedural position statement on imaging in cardiac sarcoidosis: From the Cardiovascular and Inflammation & Infection Committees of the European Association of Nuclear Medicine, the European Association of Cardiovascular Imaging, and the American. ***Eur Heart J Cardiovasc Imaging***. 2017;18(10):1073-1089.
123. Bennett MK, Gilotra NA, Harrington C, et al. Evaluation of the role of endomyocardial biopsy in 851 patients with unexplained heart failure from 2000-2009. ***Circ Hear Fail***. 2013;6(4):676-684.
124. Smedema JP, Snoep G, Van Kroonenburgh MPG, et al. Evaluation of the accuracy of gadolinium-enhanced cardiovascular magnetic resonance in the diagnosis of cardiac sarcoidosis. ***J Am Coll Cardiol***. 2005;45(10):1683-1690.
125. Vignaux O, Dhote R, Duboc D, et al. Detection of myocardial involvement in patients with sarcoidosis applying T2-weighted, contrast-enhanced, and cine magnetic resonance imaging: Initial results of a prospective study. ***J Comput Assist Tomogr***. 2002;26(5):762-767.
126. Yang Y, Safka K, Graham JJ, et al. Correlation of late gadolinium enhancement MRI and quantitative T2 measurement in cardiac sarcoidosis. ***J Magn Reson Imaging***. 2014;39(3):609-616.
127. Greulich S, Deluigi CC, Gloekler S, et al. CMR imaging predicts death and other adverse events in suspected cardiac sarcoidosis. ***JACC Cardiovasc Imaging***. 2013;6(4):501-511.
128. Hulten E, Agarwal V, Cahill M, et al. Presence of Late Gadolinium Enhancement by Cardiac Magnetic Resonance among Patients with Suspected Cardiac Sarcoidosis Is Associated with Adverse Cardiovascular Prognosis: A Systematic Review and Meta-Analysis. ***Circ Cardiovasc Imaging***. 2016;9(9):1-9.

129. Tadamura E, Yamamuro M, Kubo S, et al. Multimodality imaging of cardiac sarcoidosis before and after steroid therapy. ***Circulation***. 2006;113(20):771-773.
130. Pelliccia A, Sharma S, Gati S, et al. 2020 ESC Guidelines on sports cardiology and exercise in patients with cardiovascular disease. ***Eur Heart J***. Published online 2020:1-80.
131. Baggish AL, Wood MJ. Athlete's heart and cardiovascular care of the athlete: Scientific and clinical update. ***Circulation***. 2011;123(23):2723-2735.
132. Claessen G, Schnell F, Bogaert J, et al. Exercise cardiac magnetic resonance to differentiate athlete's heart from structural heart disease. ***Eur Heart J Cardiovasc Imaging***. 2018;19(9):1062-1070.
133. Millar LM, Fanton Z, Finocchiaro G, et al. Differentiation between athlete's heart and dilated cardiomyopathy in athletic individuals. ***Heart***. Published online 2020:1059-1065.
134. Wasfy MM, Weiner RB. Differentiating the athlete's heart from hypertrophic cardiomyopathy. ***Curr Opin Cardiol***. 2015;30(5):500-505.
135. Pelliccia A, Maron BJ, De Luca R, Di Paolo FM, Spataro A, Culasso F. Remodeling of left ventricular hypertrophy in elite athletes after long-term deconditioning. ***Circulation***. 2002;105(8):944-949.
136. Swoboda PP, Garg P, Levelt E, et al. Regression of Left Ventricular Mass in Athletes Undergoing Complete Detraining Is Mediated by Decrease in Intracellular but Not Extracellular Compartments. ***Circ Cardiovasc Imaging***. 2019;12(9):1-9.
137. Bohm P, Schneider G, Linneweber L, et al. Right and left ventricular function and mass in male elite master athletes: A controlled contrast-enhanced cardiovascular magnetic resonance study. ***Circulation***. 2016;133(20):1927-1935.
138. Sheikh N, Papadakis M, Schnell F, et al. Clinical profile of athletes with hypertrophic cardiomyopathy. ***Circ Cardiovasc Imaging***. 2015;8(7):1-9.
139. Abernethy WB, Choo JK, Hutter AM. Echocardiographic characteristics of professional football players. ***J Am Coll Cardiol***. 2003;41(2):280-284.
140. Le Grice I.J., Small B.H., Chai L.Z., Edgar S.G., Gavin J.B., Hunter P.J. . Laminar structure of the heart : ventricular myocyte arrangement and connective tissue architecture in the dog. ***Am J Physiol - Hear Circ Physiol.*** 1995;296(38):571-582.
141. Nielles-Vallespin S, Khalique Z, Ferreira PF, et al. Assessment of Myocardial Microstructural Dynamics by In Vivo Diffusion Tensor Cardiac Magnetic Resonance. ***J Am Coll Cardiol***. 2017;69(6):661-676.
142. Scollan DF, Holmes A, Winslow R, Forder J. Histological validation of myocardial microstructure obtained from diffusion tensor magnetic resonance imaging. ***Am J Physiol - Hear Circ Physiol.*** 1998;275(6 44-6):9843833.
143. Holmes AA, Scollan DF, Winslow RL. Direct Histological Validation of Diffusion Tensor MRI in Formaldehyde-Fixed Myocardium. ***Magn Reson Med***. 2000;44(1):157-161.
144. Khalique Z, Ferreira PF, Scott AD, et al. Diffusion Tensor Cardiovascular Magnetic Resonance in Cardiac Amyloidosis. ***Circ Cardiovasc Imaging***. 2020;13(5):1-11.
145. Indik JH, Gimbel JR, Abe H, et al. 2017 HRS expert consensus statement on magnetic resonance imaging and radiation exposure in patients with cardiovascular implantable electronic devices. ***Hear Rhythm***. 2017;14(7):e97-e153.
146. Royal College of Radiologists. Guidance on gadolinium-based contrast agent administration to adult patients. ***Clin Radiol***. 2019;(April):1-23. www.rcr.ac.uk